energies

Article

Transmission Expansion Planning Considering Wind Power and Load Uncertainties

Yilin Xie [1] and Ying Xu [2,*]

[1] School of Electrical Engineering and Telecommunications, The University of New South Wales, Sydney 2052, Australia
[2] School of Electrical Engineering and Automation, Harbin Institute of Technology, Harbin 150001, China
* Correspondence: ying.xu@hit.edu.cn

Abstract: Due to the rapidly increasing power demand worldwide, the development of power systems occupies a significant position in modern society. Furthermore, a high proportion of renewable energy resources (RESs) is an inevitable trend in further power system planning, due to traditional energy shortages and environmental pollution problems. However, as RESs are variable, intermittent, and uncontrollable, more challenges will be introduced in transmission expansion planning (TEP). Therefore, in order to guarantee the security and reliability of the power system, research related to TEP with the integration of RESs is of great significance. In this paper, to solve the TEP problem considering load and wind power uncertainties, an AC TEP model solved by a mixed integer non-linear programming (MINLP) is proposed, the high-quality optimal solutions of which demonstrate the accuracy and efficiency of the method. Latin hypercube sampling (LHS) is employed for the scenario generation, while a simultaneous backward reduction algorithm is applied for the scenario reduction, thus reducing the computational burden. Through this method, the reserved scenarios can effectively reflect the overall trends of the original distributions. Based on a novel worst-case scenario analysis method, the obtained optimal solutions are shown to be more robust and effective.

Keywords: transmission expansion planning; AC model; Latin hypercube sampling; scenario reduction; mixed integer non-linear programming

Citation: Xie, Y.; Xu, Y. Transmission Expansion Planning Considering Wind Power and Load Uncertainties. *Energies* **2022**, *15*, 7140. https://doi.org/10.3390/en15197140

Academic Editor: Frede Blaabjerg

Received: 26 August 2022
Accepted: 19 September 2022
Published: 28 September 2022

1. Introduction

1.1. Background

With the rapid development of technology and modern society, the power demands have been dramatically increasing all over the world. Therefore, power system planning has attracted significant attention in recent years and has become a popular topic among researchers. The transmission network occupies a necessary position in a power system, which is responsible for the delivery of power between the generation network and distribution network. Therefore, transmission expansion planning (TEP) has also become an attractive research field in recent years, and many papers have summarized the achievements of related studies. However, it must be mentioned that TEP is a decision-making process with a high complexity and different objectives, including many uncertainties such as load fluctuations and equipment faults that need to be considered in the planning process. Furthermore, a series of constraints, such as those in technical, economic, and environmental aspects, should be satisfied to guarantee the security, stability, and reliability of the power system [1].

Along with rapid economic growth, energy supply has become an important factor in determining the sustainable development of an economy. However, the massive consumption of traditional energy resources has brought obvious energy shortages and environmental problems [2,3]. As a result, renewable energy resource (RES) strategies have gained worldwide consensus, which involve increasing the employment of RESs (e.g., solar, wind) in power systems, making them cleaner, more secure, and sustainable [4–6].

A high proportion of RESs in a power system will make the network planning more complex, due to the intermittence, randomness, and uncontrollability of RESs [7]. As more uncertainties and fluctuations are added to the power system with the integration of RESs, there should be higher requirements for flexibility, reliability, and other aspects in TEP methods [8]. Therefore, research on TEP based on the characteristics of RESs are of great significance, in order to guarantee the security and stability of power systems.

1.2. Literature Review

TEP is a process of determining the time, position, and number of new devices that need to be re-built in a power system in order to provide a sufficient available capacity of the transmission network during the planning horizon [9]. TEP problems are discrete, dynamic, non-linear, multi-objective, and complex, and some technical assumptions and simplifications need to be made. According to different simplification methods, many planning models with their own characteristics have been formulated.

The main models to present simplified TEP problems are DC models, hybrid models, transportation models, and disjunctive models; for a comparison among these models, see [10–12]. When using a DC model, the non-linear equations considered in the TEP problems can be transformed into linear ones. In this way, the computational efficiency can be significantly improved [11]. However, some disadvantages still exist when a DC model is adopted. During the DC modeling process, the reactive power is ignored, such that the obtained optimal solution still needs to be followed by a separate reactive power compensation plan. Besides, the power losses are difficult to take into consideration initially and the terminal voltage magnitudes are assumed to be fixed; all of these simplifications will lead to a gap between the obtained DC model and a real operation of the AC system [13]. As a result, AC models have been developed in many studies, which take reactive power, real power losses, voltage magnitude, and phase angles into consideration [9,14–18]. An AC model has been proposed in [9], in which a high-quality optimal solution was obtained and the reactive power allocation was taken into consideration. In [14], the authors reported an ACTEP problem, which was solved through the relaxation of binary variables and determined the local optimal result. A less relaxed model has been presented in [15], which aims to yield a more realistic TEP result. In this paper, an N-1 criterion was presented in an effective method, and variables such as reactive power, terminal voltage, and power losses were presented in a linear way. It has been reported, in [16], that the non-linear ACTEP problem can be transferred into a linear one, guaranteeing the achievement of a global optimal result. In [17], a TEP problem was solved in two stages: a DC model was employed in the first stage, while an AC model was applied in the next stage, which aims to obtain an optimal solution for reactive power planning (RPP). A similar procedure has been employed in [18], with a combination of TEP followed by a RPP problem solved to provide high-quality results. In conclusion, an AC model can present a real AC grid more accurately and completely; however, there are still exist many difficulties in developing an effective solution technique to solve such a non-linear and non-convex problem.

Many different algorithms have been developed, which can be mainly divided into two types—mathematical optimization algorithms and heuristic algorithms—as well as tools named meta-heuristics, which have the characteristics of both kinds of algorithms. The basic idea of a mathematical optimization method is to transform the TEP problem into a general mathematical model, then solve it using a certain algorithm. The most common ones include linear programming (LP) [19,20], dynamic programming [21,22], nonlinear programming (NLP) [23], and mixed integer programming [20,24,25]. A technique named the Benders decomposition method has been employed in many papers [26,27], which is an effective method for small- and medium-scale power systems; however, for the large-scale systems, the huge computational burden can be a problem. Heuristic algorithms are proposed according to intuition and experience, which can provide a feasible solution for every instance of an optimization problem within the acceptable computational time. The basic idea of a heuristic method used in transmission network planning is to establish a sensitivity relationship between the decision variables and a certain validity index, then to form a new planned power network by adding and deleting candidate lines in the initial network.

In recent years, there has been greater employment of RESs in power systems, due to energy shortages and environmental pollution problems. Many methods have been proposed to deal with the uncertainties of RESs. In [28], a chance-constrained method was presented to address the TEP problem, and the wind turbine PDF was combined with a power flow analysis to obtain an optimal solution with less computational burden. A stochastic programming method has been proposed in [11], in order to express the uncertainties, and an FSA method was improved to reduce the computational burden. Another popular technology, named the scenario generation, has been widely used to obtain large numbers of scenarios [29,30]. The principle of the scenario generation is to sample known random variables which conform to a certain probability distribution. In this way, the continuous probability model can be discretized to generate a finite number of scenarios which can approximately reflect its own probability density. There are many methods for the scenario generation, such as the Monte Carlo method [28], Latin hypercube sampling [11,31,32], the scenario tree [33], and so on.

The generation of many scenarios based on uncertain parameters can lead to the significant computational burden and increase the complexity of the problem. Therefore, it is desirable to sample a subset of scenarios as the best approximation of the original ones, in order to release some of the computational burden while guaranteeing the quality of the optimal solution. This is known as an important method: the scenario reduction [34,35]. In [36], the fast forward selection (FFS) has been treated as an efficient method. It was also used to make a comparison with other methods detailed in [37], and the results indicated that the FFS can offer the optimal solution with relatively low cost and computational burden. In [38], a multi-stage model has been used for the short-term TEP problem when considering various load uncertainties. To obtain an effective and high-quality result, a Monte Carlo (MC) simulation method was employed for the scenario generation, and the GAMS/SCENRED technique was used to complete the scenario reduction process. In [11], an improved forward selection algorithm (IFSA) has been proposed for solving the stochastic TEP problem, which can save computational time while guaranteeing the accuracy of the solution.

As the scenario-based methods depend on an approximation of the real wind power and load distribution, the optimal results can be heavily affected by the representativeness of the selected scenarios. In this way, the accuracy and reliability of the planning results cannot be guaranteed [39]. Normally, to overcome the drawbacks of the scenario-based methods, the chance-constrained method is widely employed, which adds one or more constraints to be satisfied with a high probability of dealing with the uncertainties [28,40,41]. In this paper, the core idea of robust TEP is employed, which maximizes the performance of the power system under the worst-case scenario, thus ensuring the robustness and reliability of the power system [42]. Furthermore, a novel robust method is proposed to present the worst-case scenario of the power demands. Traditionally, to guarantee the safety of the power system operation, the optimal solution of TEP problems is proposed under the peak load situation, which can be considered as the worst-case scenario. When taking the integration of RESs into account, the peak load cannot be treated as the worst situation anymore, as the power generation by RESs fluctuates over time. A normal method to process the fluctuations is to average the performance of power system under all scenarios, weighted by their probabilities of appearance [43–45]. In this paper, the idea of 'net peak' is proposed in the demand analysis, which denotes the highest value of the difference between the power demands and renewable energy generation. As a result, with the additional consideration of net peak values, the security and reliability of the power system can be better guaranteed.

1.3. Contributions to the Research

The main contributions of this paper are listed as follows:

- An AC TEP model considering wind power and load uncertainties is solved using the MINLP method. High-quality optimal results are achieved with high efficiency.
- To express the uncertainties more accurately, the scenario analysis method is employed. The LHS method is used to finish the scenario generation process, where the advantages of this method include high sampling efficiency and high accuracy.
- A simultaneous backward reduction algorithm is applied for scenario reduction, which proves that the reversed scenarios can well-describe the changing characteristics of wind power generation and load fluctuations. The computational burden can be lowered, to a large extent.
- Finally, a novel method to present the worst-case scenario of power demand is proposed, which can better guarantee the security of the power system.

The remainder of this paper is organized as follows: Section 2 details the proposed AC TEP model incorporating wind power. Section 3 presents the wind uncertainties, load uncertainties, and scenario analysis. Section 4 analyses a case study using Garver's six-bus system. Section 5 highlights the conclusions and achievements of this study.

2. AC-TEP Model Incorporating Wind Power

2.1. Objective Functions

The objective of TEP is to satisfy the power demand under the most optimal transmission network structure with a minimum investment cost. The objective function can be given as follows:

$$\text{Min. } f(v) = \sum\nolimits_{(i,j)} C_{ij} \times n_{ij}, \tag{1}$$

where $f(v)$ is the total investment cost of adding transmission lines, C_{ij} is the cost of adding one transmission line between bus i and bus j, and n_{ij} denotes the number of new transmission lines which should be built between bus i and bus j. The specific data are provided in Table 1.

Table 1. Branch data.

Bus i	Bus j	r_{ij}, pu	x_{ij}, pu	Capacity (MVA)	Cost (USD M)	n_0	n_{max}
1	5	0.020	0.200	120	20	1	5
1	6	0.068	0.680	90	68	0	5
2	3	0.020	0.200	120	20	1	5
2	4	0.040	0.400	120	40	1	5
2	5	0.031	0.310	120	31	0	5
2	6	0.030	0.300	120	30	0	5
3	4	0.059	0.590	120	59	0	5
3	5	0.020	0.200	120	20	1	5
3	6	0.048	0.480	120	48	0	5
4	5	0.063	0.630	95	63	0	5
4	6	0.030	0.300	120	30	0	5
5	6	0.061	0.610	98	61	0	5

The proposed model is solved using the Yalmip optimization toolbox of MATLAB, and the MINLP method is employed to obtain the optimal solutions.

2.2. Contraints

2.2.1. Equality Constraints

Power balance equations:

For the active power:

$$P_i - P_{Gi} - P_{WTi} + P_{Di} = 0, \tag{2}$$

where P_i stands for the total active power flows out of bus i, P_{Gi} stands for the active power generated at bus i, P_{Di} stands for the demand of active power at bus i, and P_{WTi} stands for the wind power generation at bus i.

For the reactive power:

$$Q_i - Q_{Gi} + Q_{Di} = 0, \tag{3}$$

where Q_i stands for the total reactive power flows out of bus i, Q_{Gi} stands for the reactive power generated at bus i, and Q_{Di} stands for the demand of reactive power at bus i.

Following this, P_i and Q_i can be expressed as functions of the phase angle, terminal voltage, and the number of transmission lines, written as follows:

$$P_i = V_i \sum_{j \in N} V_j \left[G_{ij} cos\theta_{ij} + B_{ij} sin\theta_{ij} \right], \tag{4}$$

$$Q_i = V_i \sum_{j \in N} V_j \left[G_{ij} sin\theta_{ij} - B_{ij} cos\theta_{ij} \right], \tag{5}$$

where V_i and V_j denote the magnitude of terminal voltage at bus i and bus j, respectively; N stands for the total number of buses; and θ_{ij} stands for the voltage phase angle difference between bus i and bus j. To divide admittance elements into diagonal and non-diagonal elements, the matrices G and B can be presented as follows:

$$G = \begin{cases} G_{ij} = -\left(n_{ij} \times g_{ij} + n_{ij}^0 \times g_{ij}^0 \right) \\ G_{ii} = \sum\limits_{j \in N_{ci}} \left(n_{ij} \times g_{ij} + n_{ij}^0 \times g_{ij}^0 \right) \end{cases}, \tag{6}$$

$$B = \begin{cases} B_{ij} = -\left(n_{ij} \times b_{ij} + n_{ij}^0 \times b_{ij}^0 \right) \\ B_{ii} = \sum\limits_{j \in N_{ci}} \left(n_{ij} \times b_{ij} + n_{ij}^0 \times b_{ij}^0 \right) \end{cases}, \tag{7}$$

where g_{ij} and b_{ij} denote the conductance and susceptance, respectively, of the transmission line between bus i and bus j; n_{ij} stands for the number of new transmission lines built between bus i and bus j; n_{ij}^0 stands for the number of original transmission lines connected between bus i and bus j; and N_{ci} stands for the total number of buses connected to bus i directly.

2.2.2. Inequality Constraints

According to the requirement that the power flow in each transmission line cannot exceed its capacity, we obtain the following inequalities:

$$(n_{ij} + n_{ij}^o) \times S_{ij} \leq (n_{ij} + n_{ij}^o) \times S_{capacity}, \tag{8}$$

$$(n_{ij} + n_{ij}^o) \times S_{ji} \leq (n_{ij} + n_{ij}^o) \times S_{capacity}, \tag{9}$$

where S_{ij} stands for the apparent power flows from bus i to bus j on each transmission line and S_{ji} stands for the apparent power flows to bus j from bus i on each transmission line. The difference between these two values is the power loss. Furthermore, the apparent power flows S_{ij} and S_{ji} can be calculated as follows:

$$S_{ij} = \sqrt{\left(P_{ij}\right)^2 + \left(Q_{ij}\right)^2}, \tag{10}$$

$$P_{ij} = V_i^2 \times g_{ij} - V_i V_j \times \left(g_{ij} cos\theta_{ij} + b_{ij} sin\theta_{ij} \right), \tag{11}$$

$$Q_{ij} = -V_i^2 \times b_{ij} - V_i V_j \times \left(g_{ij} sin\theta_{ij} - b_{ij} cos\theta_{ij} \right), \tag{12}$$

$$S_{ji} = \sqrt{\left(P_{ji}\right)^2 + \left(Q_{ji}\right)^2}, \tag{13}$$

$$P_{ji} = V_j^2 \times g_{ij} - V_i V_j \times \left(g_{ij} cos\theta_{ij} - b_{ij} sin\theta_{ij}\right), \tag{14}$$

$$Q_{ji} = -V_j^2 \times b_{ij} + V_i V_j \times \left(g_{ij} sin\theta_{ij} + b_{ij} cos\theta_{ij}\right), \tag{15}$$

where P_{ij} stands for the active power flows from bus i to bus j on each transmission line, P_{ji} stands for the active power flows to bus j from bus i on each transmission line, Q_{ij} stands for the reactive power flows from bus i to bus j on each transmission line, and Q_{ji} stands for the reactive power flows to bus j from bus i on each transmission line.

2.2.3. Lower and Upper Bounds

For the generation limitation of the generators:

$$P_{Gi}^{min} \leq P_{Gi} \leq P_{Gi}^{max}\ , \tag{16}$$

$$Q_{Gi}^{min} \leq Q_{Gi} \leq Q_{Gi}^{max}, \tag{17}$$

where P_{Gi}^{min} and P_{Gi}^{max} stand for the lowest and highest active power generation capacity at bus i, and Q_{Gi}^{min} and Q_{Gi}^{max} stand for the lowest and highest reactive power generation capacity at bus i, respectively.

For the terminal voltage limitation at each bus:

$$V_i^{min} \leq V_i \leq V_i^{max}, \tag{18}$$

where V_i^{min} stands for the minimum terminal voltage magnitude, which is set as 0.95, and V_i^{max} stands for the maximum terminal voltage magnitude, which is set as 1.05.

For the limitation of the number of total transmission lines which can be connected by one bus:

$$0 \leq n_i \leq n_{max}, \tag{19}$$

where n_i stands for the number of total transmission lines connected to bus I, and n_{max} stands for the maximum number of transmission lines that can be connected to one bus.

3. Uncertainties and Scenario Analysis

3.1. Uncertainties of Wind Power and Load

To deal with the uncertainties due to the use of wind power and load fluctuations, wind speed is usually presented using a Weibull PDF and the load is modeled by a Normal PDF. The detailed models for wind generation and uncertainty analysis are described in the following.

3.1.1. Wind Uncertainties

Wind energy has the characteristics of randomness, intermittence, and uncertainty, which can be well-expressed by the wind speed probability distribution. The most popular PDF for the representation of wind speed is the Weibull distribution, which can be expressed as follows:

$$f^u = \frac{k}{c} \times \left(\frac{u}{c}\right)^{k-1} \times exp\left(-\left(\frac{u}{c}\right)^{k-1}\right),\ \forall\, c > 1\ \wedge k > 0, \tag{20}$$

$$k = \left(\frac{\sigma^u}{\mu^u}\right)^{-1.086}, \tag{21}$$

$$c = \frac{\mu^u}{\Gamma(1 + 1/k)}, \tag{22}$$

where v denotes the predicted average wind speed of the wind field, k is the shape factor, and c is the scale factor, which can reflect the range and extent of wind speed fluctuations.

The principle of a wind turbine is to convert mechanical energy into electrical energy. The output power of a wind turbine is highly dependent on the wind speed, and the function and curve (shown in Figure 1) describing wind generation are given as follows:

$$P_{WT}(v) = \begin{cases} 0, when\ v < v_{ci}\ \&\ v > v_{co} \\ P_{rate}\left(\frac{v - v_{ci}}{v_{rate} - v_{ci}}\right), when\ v_{ci} \le v \le v_{rate}, \\ P_{rate}, when\ v_{rate} \le v \le v_{co} \end{cases} \tag{23}$$

where P_{WT} is the output power of each wind turbine, v_{ci} stands for the cut-in wind speed (which is set as 3 m/s), v_{rate} stands for the rated wind speed (which is set as 12 m/s), v_{co} stands for the cut-off wind speed (which is set as 25 m/s), and P_{rate} stands for the rated output power of each wind turbine [13]. The TEP solution was proposed based on Garver's network, the total power generation capacity by fossil fuels was 1110 MW, and the total wind turbine generation capacity was assumed as 370 MW (i.e., one-third of the fossil fuel generation capacity).

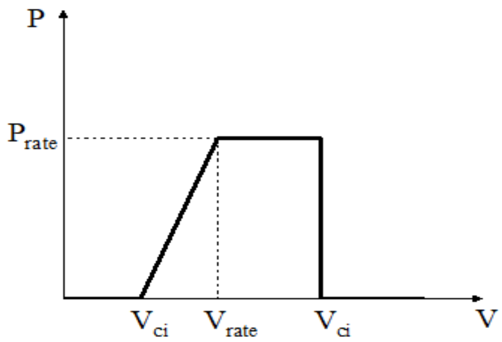

Figure 1. The relationship between wind speed and power generation.

3.1.2. Load Uncertainties

The load side occupies a significant position in a power system, and load fluctuations can have a serious effect on the voltage stability. Power system planning, operation, and control all aiming at ensuring the security of the load supply. As a result, it is of great significance to deal with load uncertainties in a power system analysis.

However, the load demand typically presents a periodic change, according to the regular change of production and life order. At the same time, the change of load is random and fluctuates, and can be affected by many uncertain factors, such as the economy, society, and weather. Particularly, the load growth is directly related to the economic growth, which is also extremely hard to estimate. As a result, experts in the field of economics have formulated propositions according to their experience. In this light, a normal PDF can be employed to present the load uncertainties, shown as follows [46]:

$$f_d(P_d) = \frac{1}{\sigma_d\sqrt{2\pi}} \exp\left[-\frac{(P_d - \mu_d)^2}{2\sigma_d^2}\right], \tag{24}$$

where μ_d and σ_d stand for the mean and standard deviation, and P_d denotes the probability density of a normally distributed load.

3.2. Scenario Analysis

A Scenario analysis is a common method to describe TEP problems considering uncertainty and randomness. In order to guarantee the security and stability of a power system, a scenario analysis has been widely applied to address the uncertainties brought by RESs and load fluctuations, which can be considered a significant aspect of TEP.

The key point of applying a scenario analysis method is balancing the computational efficiency and accuracy: if the number of generated scenarios is too large, the huge computational burden will lead to low efficiency; in contrast, if a small number of scenarios are generated, the accuracy cannot be guaranteed. As a result, scenario analysis methods are divided into two aspects: the first is the scenario generation technology, which is used to generate a large amount of scenarios to guarantee the computational accuracy, while the second is a scenario reduction technology, which is used to reduce the number of scenarios to guarantee computational efficiency.

In this study, Latin hypercube sampling (LHS) is employed to generate scenarios and express uncertainties. Meanwhile, a simultaneous backward reduction algorithm is proposed to carry out the scenario reduction process. In this way, both computational accuracy and efficiency can be guaranteed.

3.2.1. Scenario Generation: LHS

According to the PDF of wind speed and load, LHS is applied to obtain many scenarios and obtain an approximate description of the uncertainties.

Latin hypercube sampling (LHS) is composed of two parts: sampling and sorting. Its simulation accuracy is affected by the correlation between the sampled values and the different input random variables. The basic requirement of the sampling process is to have the sampling points of the input random variables completely cover their randomly distributed areas. The sorting process aims to control the correlation among the sampled values of the input variables; in this way, the impact of the correlation among sampled values on the accuracy of LHS can be reduced. Compared with simple random sampling, the advantages of LHS are its high efficiency and good robustness.

LHS is a stratified sampling technique, and the sampled values from this method can reflect the whole distribution of input random variables effectively. In comparison with the traditional Monte Carlo method, its advantage that the sampled points can cover the whole sampling area. In contrast, the random sampling method employs the Monte Carlo sampling (MCS) technique, which means that, within the sampling area, the sampled values may fall at any position. As a result (especially for small-scale sampling), the output probability distribution may become aggregated. As a result, the scenarios obtained by the LHS method are more representative of the distribution. At the same time, the computational efficiency and accuracy can be improved, to some extent.

(1) Sampling Process

It is assumed that $x_1, x_2, \ldots, x_K$ are k input random variables in the probability problem to be solved, and x_K is any random variable of $x_1, x_2, \ldots, x_K$, whose cumulative probability distribution function can be expressed as:

$$Y_K = F_K(x_K). \tag{25}$$

It is supposed that N is the sampling scale, and the sampling method can be carried out as follows: divide the vertical axis of the curve $Y_K = F_K(x_K)$ into N equally spaced non-overlapping intervals and select one sampled value from each interval (the selected point can be random or the midpoint of each interval). In our search, the midpoint of each interval was chosen; this sampling method is called "lattice sampling". Then, use the inverse function of $Y_K = F_K(x_K)$ to express the sampled value of x_K. The nth sample value of x_K can be expressed as:

$$x_{Kn} = F_k^{-1}\left(\frac{n-0.5}{N}\right). \tag{26}$$

The sampled values of the random variable x_K are arranged in a row of the sampling matrix, denoted as $[x_{K1} \ldots x_{Kn} \ldots x_{KN}]$. When the sampling processes of K input random variables are finished, all of the sample values can be formed into a $K \times N$ initial sampling matrix X_s. Then, the next step of the LHS method should be applied; that is, arranging the order of the sample points of each row and eliminating the correlation between the rows of X_s.

(2) Sorting Process

The sorting process aims to minimize the correlation between the rows of the matrix X_s, as the correlation between the sampled values and the different input random variables is difficult to control and can have an effect on the calculation accuracy. A high-quality sorting method is very important for reducing the correlation between the rows of the sampling matrix and improving the efficiency and accuracy of LHS. In this way, a Cholesky decomposition method is employed in this section, which has the advantages of high efficiency and low computational burden.

The first step in rearranging the sampling matrix X_s using the Cholesky decomposition method is to initialize a $K \times N$ matrix $L = [L_{1,}\ldots,\ L_k]^T$, where each row of L consists of a random arrangement of integers 1, ..., N. It is assumed that the correlation coefficients between the rows of the matrix L can be expressed by a positive definite symmetric matrix ρ_L, and the Cholesky decomposition method is applied to obtain a non-singular lower triangular matrix D which satisfies the following equation:

$$\rho_L = DD^T. \tag{27}$$

Then, a matrix G of dimensions $K \times N$ can be obtained, whose correlation coefficient matrix is a unit matrix of dimensions $K \times K$:

$$G = D^{-1}L. \tag{28}$$

Unlike the matrix L, not all of the values in G are integers, such that they cannot be used to show the positions of elements in the sampling matrix. Therefore, the row elements of L are replaced by the elements in G, which are arranged in order from large to small. Then, the element positions in each row of X_s are transferred, which are indicated by the elements in the corresponding row of the updated matrix L. As the correlation coefficients of G form an identity matrix, the rows of G are irrelevant. When each row's elements of the new matrix L are replaced by the elements in the corresponding row of G, in order from large to small, the correlations between different elements will be reduced, compared with those in the original matrix L.

Assume that ρ_x is the matrix of the correlation coefficients after X_s is rearranged. It should be noted that, after the data in X_s are rearranged according to L, $\rho_{L,}$ and ρ_x have the characteristic of consistency, but are not completely equal. As ρ_L is a rank correlation matrix, the smaller values of the elements in the matrix ρ_L will lead to smaller values of the elements in ρ_x.

It should be mentioned that the sampling technique is not necessary to apply initially during the calculation process. An alternative method can be considered for generating L first, and then the values of the sampling matrix can be calculated by the following method:

$$[x_{k1}, \ldots, x_{kN}] = F_k^{-1}\left(\frac{L_k - 0.5}{N}\right). \tag{29}$$

As L is no longer used in subsequent calculations, it can be overwritten with the generated sampling matrix X_s, in order to save memory.

The elements in each row of the sampling matrix X_s represent the sampled values of each random variable, and the elements in each column represent the input values of each random variable in one random simulation process.

3.2.2. Scenario Reduction: Simultaneous Backward Reduction Method

In the scenario generation process, many random scenarios will be generated with an equal probability, which can lead to a heavy computational burden. However, many of the generated scenarios are similar—from the perspective of the amount of information that they can provide—and there is little significance of precise research on them. As a result, a scenario reduction process seems necessary, which aims at selecting fewer classical and representative scenarios from many real historical ones, following which the reproduced probabilities are arranged with respect to the chosen scenarios, in order to span the largest range of original outcomes. In this way, both the accuracy and efficiency can be guaranteed during the scenario analysis process.

The scenario reduction technique can be expressed through the concept of distance. The distance between the scenes $i(t)$ and $j(t)$ defined at time point t can be represented as follows:

$$\mathrm{c}_t\left(p_{g\omega}^{i(t)}, p_{g\omega}^{j(t)}\right) = \|p_{g\omega}^{i(t)} - p_{g\omega}^{j(t)}\|_2,\ t = 1,\ L, T. \tag{30}$$

The objective of the scene reduction is to minimize the distance between the original scenarios and the subset of scenarios after the reduction process; that is, under the condition that a certain number of scenarios needs to be deleted, the value of the following expression should be minimized:

$$\sum_{i\in J} p_i \cdot \min_{j\notin J} c_T\left(p_{g\omega}^i, p_{g\omega}^j\right), \tag{31}$$

where J is a set of scenarios which are eliminated in the scene reduction process, and the probabilities of scenarios i and j occurring are p_i and p_j, respectively.

In order to minimize the value of the above equation, a simultaneous backward reduction method is employed. The steps of the scenario reduction process are as follows:

(1) Let k = 0, and set the deleted scenarios $J = J^{(0)}$ as an empty set;
(2) Calculate the number of scenarios lk which need to be deleted at the kth iteration. When l is taken as lk, the value of the following equation should be minimized.

$$\sum_{i\notin J^{(k-1)}U} p_i \cdot \min_{j\notin J^{(k-1)}U} c_T\left(p_{g\omega}^i, p_{g\omega}^j\right) \tag{32}$$

(3) Delete scenarios lk, set $k = k + 1$;
(4) Set $J = J(k)$. The deleted scenarios i of J will be replaced by scenario j, which are closest to i in the retained scenarios. As a result, the probability of the remaining scenario j needs to be corrected, which should be expressed as the sum of its original probability p_j and the total probability of the deleted scenarios which are replaced by it; that is, $q_i = p_j + \sum p_i$.

The simultaneous backward reduction method is a typical scenario reduction analysis method, as both the computational efficiency and the changing characteristics of the research objects can be considered effectively. Through this technique, the generated scenarios of wind power generation and load are reduced. The scenario generation and scenario reduction processes are shown in Figure 2.

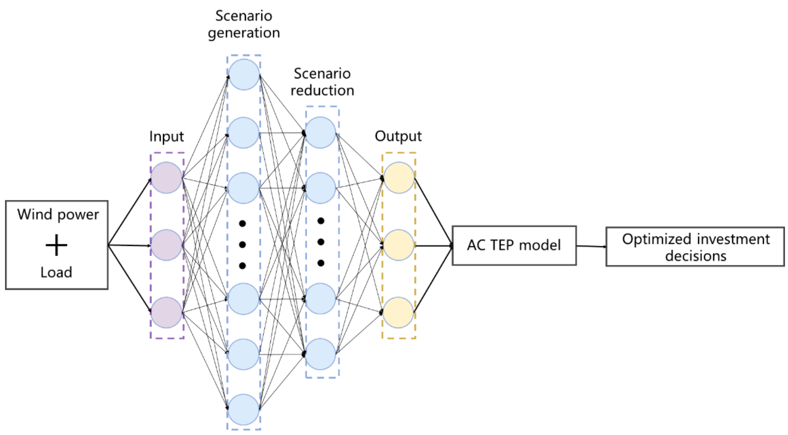

Figure 2. Flow diagram of the algorithm.

4. Case Study

4.1. Garver's Six-Bus System

The proposed model was applied to Garver's network, which consists of six buses, five loads, and three generators. There are total of 15 positions to develop the transmission network (shown in Figure 3). Originally, the demands of five loads were 20 MW, 60 MW, 10 MW, 40 MW, and 60 MW. The maximum generation capacities of the three generators at bus 1, bus 3, and bus 6 were 150 MW, 360 MW, and 600 MW, respectively. The total maximum generation capacity was 1110 MW, but bus 6 was isolated from other buses. Next, it was assumed that all demands increased by four times; in this way, the generators at bus 1 and bus 3 cannot satisfy the demand anymore, and new transmission lines need to be built to satisfy the larger power flow demand.

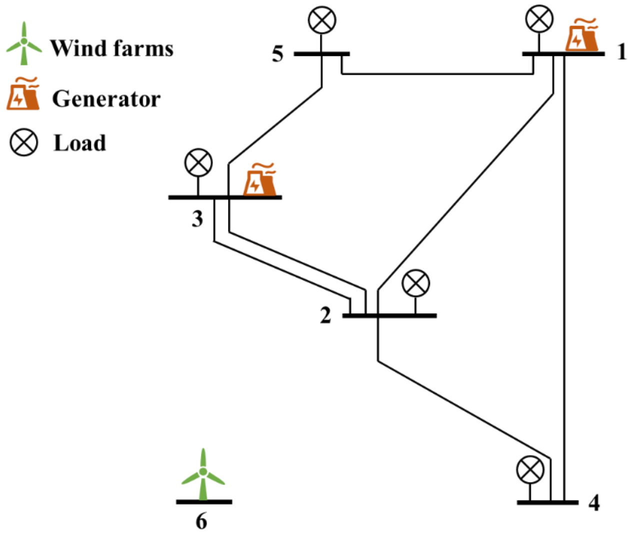

Figure 3. Flow diagram for the wind power generation based on LHS.

The basic parameters of the proposed network are given in the following tables. Table 2 shows the power demand at each bus and power generation capacity of each generator.

Table 2. Garver's six-bus system data.

Bus	Demand		Generation			
	P (MW)	Q (MVAr)	P_{MAX} (MW)	P_{MIN} (MW)	Q_{MAX} (MVAr)	Q_{MIN} (MVAr)
1	80	16	160	0	48	−10
2	240	48	\	\	\	\
3	40	8	370	0	101	−10
4	160	32	\	\	\	\
5	240	48	\	\	\	\
6	0	0	610	0	183	−10

4.2. Result of the Scenario Analysis

Wind speed is an important parameter, serving as the input of the wind turbine. The distribution of the typical wind speed per hour for one day collected from [47] is shown in Figure 4, which was taken as the input of the Weibull distribution function for the scenario generation.

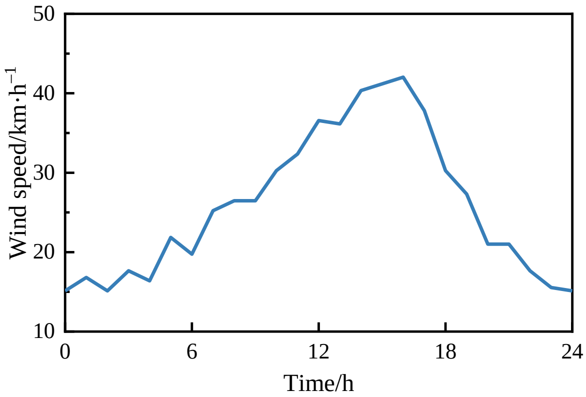

Figure 4. Daily wind speed curve.

The real load data of three hundred households has been given in [48], and four typical (postcode:2010) days in different seasons were selected to represent the daily load change. The corresponding curves are depicted in Figure 5, which show that the load demand presented seasonal variation characteristics; namely, the power demand in summer and winter was larger, compared with that in other seasons. In order to obtain a more accurate prediction result for the load data, the average seasonal power demand per day was used to simulate the load distribution on Garver's network. The obtained data were taken as the input to a normal PDF for the scenario generation.

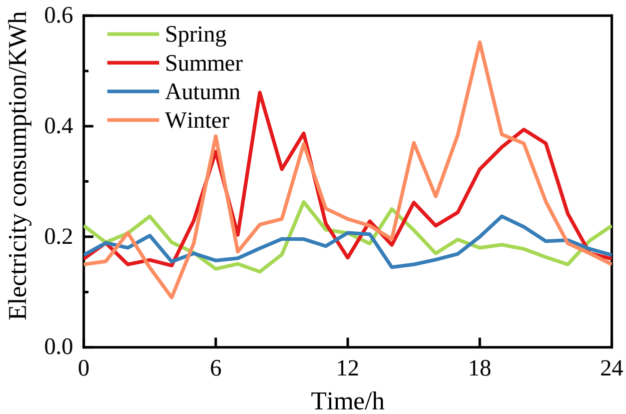

Figure 5. Daily load consumption curves in the different seasons.

When considering the TEP problem, including the uncertainties of wind energy and load fluctuations, in the first scenario generation process, the LHS technique was used to generate 4000 original wind power generation and load scenarios. Then, the scenario reduction technology (i.e., simultaneous backward reduction) was employed to reduce the number of scenarios from 4000 to 100, 100 to 10, and 10 to 3. The scenario reduction process is clearly depicted in Figure 6.

During the scenario reduction process, the scenarios with a lower probability were merged into the scenarios with a higher probability. As a result, the remaining three scenarios represent the original scenarios with the highest probability. The effectiveness and accuracy of considering the uncertainties can be guaranteed.

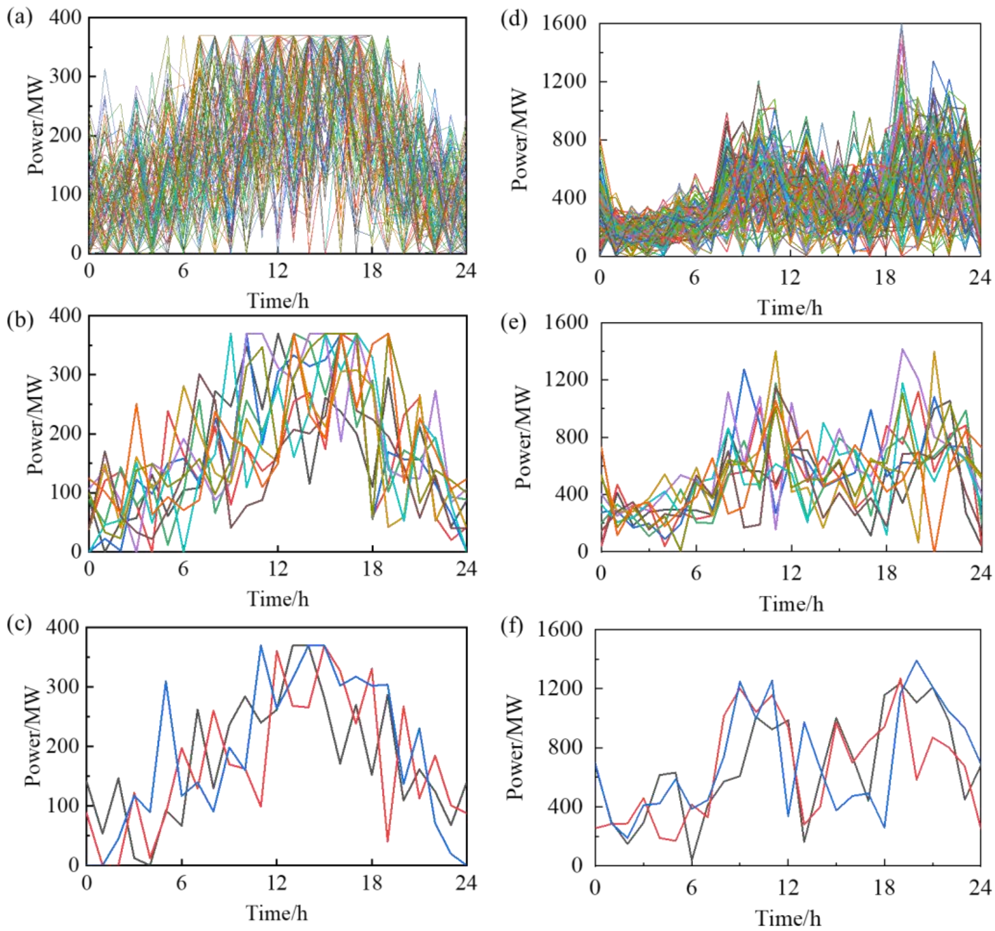

Figure 6. Scenario reduction process, regarding wind power and load scenarios: (**a**) 100 scenarios of wind power; (**b**) 10 scenarios of wind power; (**c**) 3 scenarios of wind power; (**d**) 100 scenarios of load; (**e**) 10 scenarios of load; and (**f**) 3 scenarios of load.

4.3. Optimization Results

Traditionally, to guarantee safe power system operations, the optimal solution of TEP problems is proposed under the peak load situation, which can be considered as the worst-case scenario. When taking the integration of RESs into account, the peak load cannot be treated as the worst situation anymore, as the power generation by RESs fluctuates over time. This means that, when the power demand achieves a peak value, there could be a relatively large renewable energy generation, and the scenario under a high off-peak demand value and a low RES generation should be considered as a worse case. In this way, the idea of 'net peak' is proposed in the demand analysis, which denotes the highest value of the difference between the power demand and renewable energy generation. As a result, with the additional consideration of net peak values, the security and reliability of the power system can be guaranteed, which is of great significance in TEP.

Following the scenario reduction technique, three scenarios of wind power generation distribution and three scenarios of load distribution were reserved; that is, the worst-case analysis was based on a total of nine (3×3) scenarios.

In Table 3, the parameters obtained for the nine scenarios are given, which are sorted in terms of probability, from high to low; it should be noted that the sum of all scenario probabilities is equal to one (or 100%). The nine scenarios are also shown in Figure 7, including three curves in each figure, which stand for wind power generation, load power consumption, and net load, respectively. It is shown, through the marked points, that the peak load point does not always stand for the worst-case scenario, as the largest net load value is under the net peak case. In this way, the new idea of a worst-case analysis considering both peak load value and net peak value proposed in this section can better ensure the security and reliability of the power system.

Table 3. Net load based on nine reduced scenarios.

	Possibility of Scenario (%)	Demand (MW)	Wind Power Generation (MW)	Net Peak Value (MW)
1	22.46	1270.419	304.175	966.244
2	16.18	1207.873	230.626	977.247
3	13.89	1270.419	287.195	983.224
4	10.61	1270.419	296.187	974.232
5	10.00	1237.604	304.175	933.429
6	9.26	1237.604	287.195	950.409
7	6.67	1116.723	190.735	925.988
8	6.56	1201.549	236.620	964.929
9	4.37	1156.879	240.343	916.536

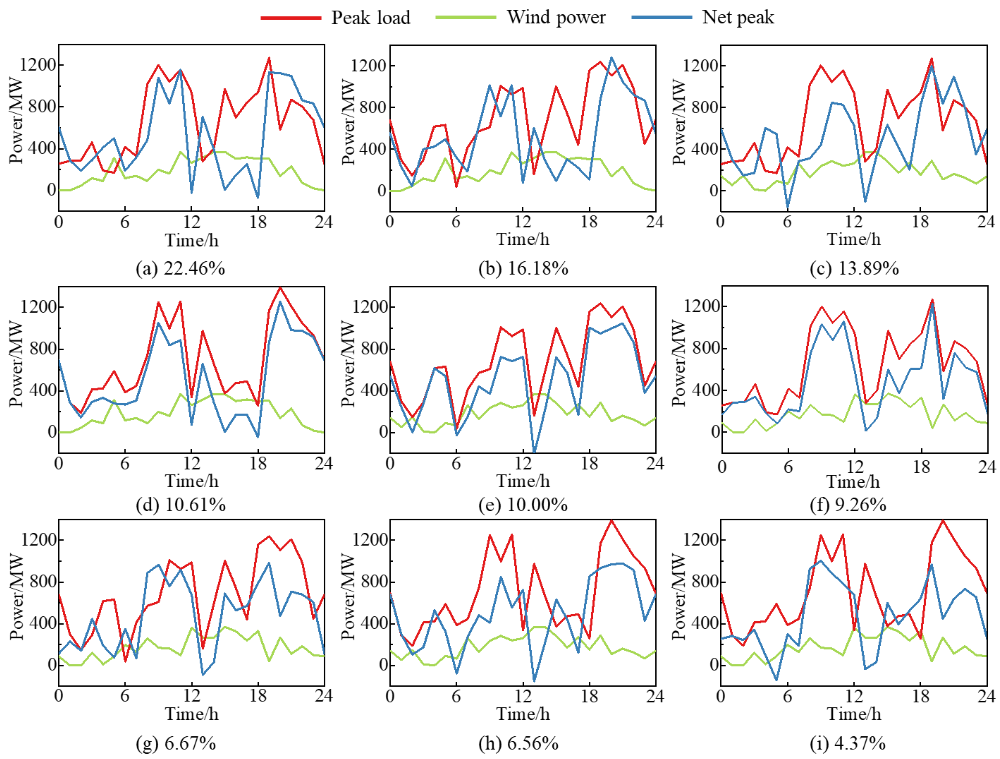

Figure 7. Net load under the different scenarios: (**a**) 22.46%; (**b**) 16.18%; (**c**) 13.89%; (**d**) 10.61%; (**e**) 10.00%; (**f**) 9.26%; (**g**) 6.67%; (**h**) 6.56%; and (**i**) 4.37%.

We can see that, based on the nine scenarios, scenario 3 should be considered as the worst-case scenario, which had the largest net peak value (of 983.224 MW). To ensure the safety of the power system, the data of the worst-case scenario was taken as the input to the proposed AC model, in order to obtain an optimal result. It is shown that the minimum investment cost of new transmission lines is USD 250 million, and the final planning scheme is $n_{12} = 1$, $n_{14} = 1$, $n_{15} = 1$, $n_{23} = 1$, $n_{24} = 1$, $n_{26} = 4$, $n_{35} = 3$, $n_{46} = 3$. The new transmission lines that need to be added are detailed in Table 4 and Figure 8.

Table 4. Optimal results based on nine reduced scenarios.

$f(v)$	Number of New Transmission Lines	Cost of Each Transmission (USD M)
USD 250 M	$n_{26} = 4$	30
	$n_{35} = 2$	20
	$n_{46} = 3$	30

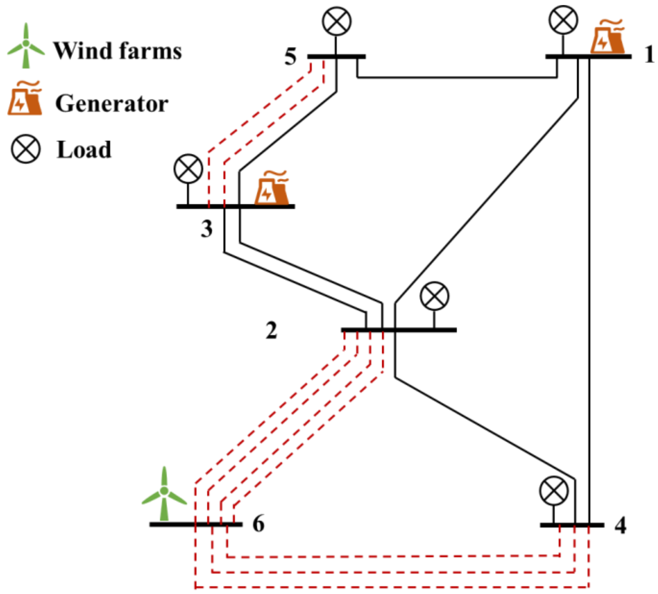

Figure 8. Optimal results for Garver's 6-bus system.

Compared to the risk-averse TEP model and deterministic security-constrained TEP model proposed in [49], the cost obtained in this study was reduced by 16.7% and 30.3%, respectively. Compared to the chance-constrained model proposed in [28], the cost was reduced by 19.2%. The optimal results obtained here prove that the combination of robust TEP and a scenario-based method not only can guarantee the security of power system operations, but can also reduce the required investment, to some extent.

To further study the impact of the reserved number of typical scenarios on the optimal results, the number of reserved scenarios was adjusted, and the optimal solutions, based on 4×4, 6×6, 8×8, and 10×10 scenarios, are provided in Table 5. For example, the expression for the 4×4 scenarios means that, during the scenario reduction process, the original 4000 scenarios were reduced to four typical scenarios each for wind power generation and load.

Table 5. Optimal results under the different number of scenarios.

	Net Peak (MW)	Scheme	Cost (USD M)
3×3	983.244	$n_{12}=1,\ n_{14}=1,\ n_{15}=1,\ n_{23}=1,$ $n_{24}=1,\ n_{26}=4,\ n_{35}=3,\ n_{46}=3$	250
4×4	1012.456	$n_{12}=1,\ n_{14}=1,\ n_{15}=1,\ n_{23}=1,$ $n_{24}=1,\ n_{26}=5,\ n_{35}=4,\ n_{46}=2$	270
6×6	1046.371	$n_{12}=1,\ n_{14}=1,\ n_{15}=1,\ n_{23}=1,$ $n_{24}=1,\ n_{26}=5,\ n_{35}=4,\ n_{46}=3$	300
8×8	1031.641	$n_{12}=1,\ n_{14}=1,\ n_{15}=1,\ n_{23}=1,$ $n_{24}=1,\ n_{26}=4,\ n_{35}=4,\ n_{46}=4$	300
10×10	1079.168	$n_{12}=1,\ n_{14}=1,\ n_{15}=1,\ n_{23}=1,$ $n_{24}=1,\ n_{26}=5,\ n_{35}=5,\ n_{46}=4$	350

According to the optimal solutions shown in the table, we can see that, with an increasing number of reduced scenarios, the net peak values generally show an upward trend and the investment costs of the optimal solutions also increase. This can be explained as, under a larger number of reduced scenarios, more extreme situations are taken into consideration and more power needs to be transferred between different buses to satisfy the fluctuating power demand. In this way, when a relatively larger number of scenarios are reduced, the higher accuracy and robustness of the power system can be achieved, while also leading to a heavy computational burden and high investment cost. In contrast, with a relatively smaller number of reduced scenarios, the computational efficiency can be improved and the investment cost can be reduced, but more operational risks must be taken.

5. Conclusions

In this paper, we proposed a comprehensive AC TEP model considering wind power and load uncertainties. Differing from the traditional random sampling technique, the LHS method was employed to complete the scenario generation process, where the advantages of this method include a high sampling efficiency and accuracy. Furthermore, a simultaneous backward reduction algorithm was applied for the scenario reduction, in order to reduce the computational complexity. A novel method was proposed to present the worst-case power demand scenario, which can better guarantee the security of a power system, compared with the traditional method. A case study conducted on Garver's six-bus system demonstrated the effectiveness and robustness of the proposed method. The main conclusions in this paper are listed as follows:

- The combination of the scenario generation and reduction methods can well-describe the changing characteristics of wind power generation and load fluctuations. A high-quality scenario analysis process can be presented, while taking the uncertainties into consideration.
- All possible extreme scenarios can be fully represented by the applied worst-case scenario method. The optimal solutions can demonstrate the impacts of uncertainties on the planning scheme, and planners should balance the investment cost and overloading risk carefully before making their final decisions.
- Compared to the proposed risk-averse and security-constrained TEP model, the planning cost was reduced by 16.7% and 30.3%, respectively, indicating the economic advantages of the proposed method.

In conclusion, the above optimal results indicate that the final optimal solution of TEP with the integration of RESs may be greatly affected by uncertain factors. TEP problems considering various uncertainties play a significant role in guaranteeing the safety of power system operations.

Author Contributions: Y.X. (Yilin Xie) did the simulation work, proposed the model solution, programmed the code and wrote the manuscript. Y.X. (Ying Xu) checked the model and proofread the manuscript. All authors have read and agreed to the published version of the manuscript.

Funding: This research received no external funding.

Conflicts of Interest: The authors declare no conflict of interest.

References

1. Mahdavi, M.; Antunez, C.S.; Ajalli, M.; Romero, R. Transmission expansion planning: Literature review and classification. *IEEE Syst. J.* **2018**, *13*, 3129–3140. [CrossRef]
2. Bertram, C.; Luderer, G.; Pietzcker, R.C.; Schmid, E.; Kriegler, E.; Edenhofer, O. Complementing carbon prices with technology policies to keep climate targets within reach. *Nat. Clim. Chang.* **2015**, *5*, 235–239. [CrossRef]
3. Olabi, A.G.; Onumaegbu, C.; Wilberforce, T.; Ramadan, M.; Abdelkareem, M.A.; Alami, A.H.A. Critical review of energy storage systems. *Energy* **2021**, *214*, 22. [CrossRef]
4. Das, P.; Mathur, J.; Bhakar, R.; Kanudia, A. Implications of short-term renewable energy resource intermittency in long-term power system planning. *Energy Strategy Rev.* **2018**, *22*, 1–15. [CrossRef]
5. Wlodarczyk, B.; Firoiu, D.; Ionescu, G.H.; Ghiocel, F.; Szturo, M.; Markowski, L. Assessing the sustainable development and renewable energy sources relationship in eu countries. *Energies* **2021**, *14*, 2323. [CrossRef]
6. Magazzino, C.; Mele, M.; Schneider, N. A machine learning approach on the relationship among solar and wind energy production, coal consumption, gdp, and CO_2 emissions. *Renew. Energy* **2021**, *167*, 99–115. [CrossRef]
7. Denholm, P.; Hand, M. Grid flexibility and storage required to achieve very high penetration of variable renewable electricity. *Energy Policy* **2011**, *39*, 1817–1830. [CrossRef]
8. Belderbos, A.; Delarue, E. Accounting for flexibility in power system planning with renewables. *Int. J. Electr. Power Energy Syst.* **2015**, *71*, 33–41. [CrossRef]

9. Rider, M.; Garcia, A.; Romero, R. Power system transmission network expansion planning using ac model. *IET Gener. Transm. Distrib.* **2007**, *1*, 731–742. [CrossRef]
10. Romero, R.; Monticelli, A.; Garcia, A.; Haffner, S. Test systems and mathematical models for transmission network expansion planning. *IEEE Proc. Gener. Transm. Distrib.* **2002**, *149*, 27–36. [CrossRef]
11. Zhan, J.; Chung, C.; Zare, A. A fast solution method for stochastic transmission expansion planning. *IEEE Trans. Power Syst.* **2017**, *32*, 4684–4695. [CrossRef]
12. Moradi-Sepahvand, M.; Amraee, T. Hybrid ac/dc transmission expansion planning considering hvac to hvdc conversion under renewable penetration. *IEEE Trans. Power Syst.* **2021**, *36*, 579–591. [CrossRef]
13. Gomes, P.V.; Saraiva, J.T.; Carvalho, L.; Dias, B.; Oliveira, L.W. Impact of decision-making models in transmission expansion planning considering large shares of renewable energy sources. *Electr. Power Syst. Res.* **2019**, *174*, 105852. [CrossRef]
14. Zhang, H.; Heydt, G.T.; Vittal, V.; Mittelmann, H.D. Transmission expansion planning using an ac model: Formulations and possible relaxations. In Proceedings of the IEEE Power and Energy Society General Meeting, San Diego, CA, USA, 22–26 July 2012; pp. 1–8.
15. Zhang, H.; Heydt, G.T.; Vittal, V.; Quintero, J. An improved network model for transmission expansion planning considering reactive power and network losses. *IEEE Trans. Power Syst.* **2013**, *28*, 3471–3479. [CrossRef]
16. Akbari, T.; Bina, M.T. A linearized formulation of ac multi-year transmission expansion planning: A mixed-integer linear programming approach. *Electr. Power Syst. Res.* **2014**, *114*, 93–100. [CrossRef]
17. Asadamongkol, S.; Eua-arporn, B. Transmission expansion planning with ac model based on generalized benders decomposition. *Int. J. Electr. Power Energy Syst.* **2013**, *47*, 402–407. [CrossRef]
18. Rahmani, M.; Rashidinejad, M.; Carreno, E.; Romero, R. Efficient method for ac transmission network expansion planning. *Electric Power Syst. Res.* **2010**, *80*, 1056–1064. [CrossRef]
19. Alizadeh, B.; Dehghan, S.; Amjady, N.; Jadid, S.; Kazemi, A. Robust transmission system expansion considering planning uncertainties. *IET Gener. Transm. Distrib.* **2013**, *7*, 1318–1331. [CrossRef]
20. Macedo, L.H.; Montes, C.V.; Franco, J.F.; Rider, M.J.; Romero, R. Milp branch flow model for concurrent ac multistage transmission expansion and reactive power planning with security constraints. *IET Gener. Transm. Distrib.* **2016**, *10*, 3023–3032. [CrossRef]
21. Alizadeh, B.; Jadid, S. A dynamic model for coordination of generation and transmission expansion planning in power systems. *Int. J. Electr. Power Energy Syst.* **2015**, *65*, 408–418. [CrossRef]
22. Wu, Z.; Zeng, P.; Zhang, X.-P. Two-stage stochastic dual dynamic programming for transmission expansion planning with significant renewable generation and nk criterion. *CSEE J. Power Energy Syst.* **2016**, *2*, 3–10. [CrossRef]
23. Ziaee, O.; Alizadeh-Mousavi, O.; Choobineh, F.F. Co-optimization of transmission expansion planning and tcsc placement considering the correlation between wind and demand scenarios. *IEEE Trans. Power Syst.* **2017**, *33*, 206–215. [CrossRef]
24. Han, S.; Kim, H.J.; Lee, D. A long-term evaluation on transmission line expansion planning with multistage stochastic programming. *Energies* **2020**, *13*, 1899. [CrossRef]
25. Haghighat, H.; Zeng, B. Bilevel mixed integer transmission expansion planning. *IEEE Trans. Power Syst.* **2018**, *33*, 7309–7312. [CrossRef]
26. Binato, S.; Pereira, M.V.F.; Granville, S. A new benders decomposition approach to solve power transmission network design problems. *IEEE Trans. Power Syst.* **2001**, *16*, 235–240. [CrossRef]
27. Moulin, L.S.; Poss, M.; Sagastizábal, C. Transmission expansion planning with re-design. *Energy Syst.* **2010**, *1*, 113–139. [CrossRef]
28. Yu, H.; Chung, C.; Wong, K.; Zhang, J.H. A chance constrained transmission network expansion planning method with consideration of load and wind farm uncertainties. *IEEE Trans. Power Syst.* **2009**, *24*, 1568–1576. [CrossRef]
29. Khan, N.H.; Jamal, R.; Ebeed, M.; Kamel, S.; Zeinoddini-Meymand, H.; Zawbaa, H.M. Adopting scenario-based approach to solve optimal reactive power dispatch problem with integration of wind and solar energy using improved marine predator algorithm. *Ain Shams Eng. J.* **2022**, *13*, 101726. [CrossRef]
30. Dong, W.; Chen, X.; Yang, Q. Data-driven scenario generation of renewable energy production based on controllable generative adversarial networks with interpretability. *Appl. Energy* **2022**, *308*, 118387. [CrossRef]
31. Ma, Z.; Gao, J.; Hu, W.; Dinavahi, V. Risk-adjustable stochastic schedule based on sobol augmented latin hypercube sampling considering correlation of wind power uncertainties. *IET Renew. Power Gener.* **2021**, *15*, 2356–2367. [CrossRef]
32. Sun, X.; Li, X.; Datta, S.; Ke, X.; Huang, Q.; Huang, R.; Hou, Z.J. Smart sampling for reduced and representative power system scenario selection. *IEEE Open Access J. Power Energy* **2021**, *8*, 293–302. [CrossRef]
33. Growe-Kuska, N.; Heitsch, H.; Romisch, W. Scenario reduction and scenario tree construction for power management problems. In Proceedings of the IEEE Bologna Power Tech Conference Proceedings, Bologna, Italy, 23–26 June 2003; Volume 3, p. 7.
34. Li, Z.; Floudas, C.A. Optimal scenario reduction framework based on distance of uncertainty distribution and output performance: I. Single reduction via mixed integer linear optimization. *Comput. Chem. Eng.* **2014**, *70*, 50–66. [CrossRef]
35. Bukenberger, J.P.; Webster, M.D. Approximate latent factor algorithm for scenario selection and weighting in transmission expansion planning. *IEEE Trans. Power Syst.* **2020**, *35*, 1099–1108. [CrossRef]
36. Feng, Y.; Ryan, S.M. Solution sensitivity-based scenario reduction for stochastic unit commitment. *Comput. Manag. Sci.* **2016**, *13*, 29–62. [CrossRef]
37. Dvorkin, Y.; Wang, Y.; Pandzic, H.; Kirschen, D. Comparison of scenario reduction techniques for the stochastic unit commitment. In Proceedings of the IEEE PES General Meeting | Conference & Exposition, Harbor, MD, USA, 27–31 July 2014; pp. 1–5.

38. Akbari, T.; Rahimikian, A.; Kazemi, A. A multi-stage stochastic transmission expansion planning method. *Energy Convers. Manag.* **2011**, *52*, 2844–2853. [CrossRef]
39. Liang, Z.; Chen, H.; Wang, X.; Ibn Idris, I.; Tan, B.; Zhang, C. An extreme scenario method for robust transmission expansion planning with wind power uncertainty. *Energies* **2018**, *11*, 2116. [CrossRef]
40. Qiu, J.; Dong, Z.Y.; Zhao, J.; Xu, Y.; Luo, F.; Yang, J. A risk-based approach to multi-stage probabilistic transmission network planning. *IEEE Trans. Power Syst.* **2016**, *31*, 4867–4876. [CrossRef]
41. Hong, S.; Cheng, H.; Zeng, P. An n-k analytic method of composite generation and transmission with interval load. *Energies* **2017**, *10*, 168. [CrossRef]
42. Akhavizadegan, F.; Wang, L.; McCalley, J. Scenario selection for iterative stochastic transmission expansion planning. *Energies* **2020**, *13*, 1203. [CrossRef]
43. Bagheri, A.; Wang, J.; Zhao, C. Data-driven stochastic transmission expansion planning. *IEEE Trans. Power Syst.* **2016**, *32*, 3461–3470. [CrossRef]
44. Liu, Y.; Sioshansi, R.; Conejo, A.J. Multistage stochastic investment planning with multiscale representation of uncertainties and decisions. *IEEE Trans. Power Syst.* **2017**, *33*, 781–791. [CrossRef]
45. Park, H.; Baldick, R.; Morton, D.P. A stochastic transmission planning model with dependent load and wind forecasts. *IEEE Trans. Power Syst.* **2015**, *30*, 3003–3011. [CrossRef]
46. Hassan, M.H.; Kamel, S.; El-Dabah, M.A.; Khurshaid, T.; Dominguez-Garcia, J.L. Optimal reactive power dispatch with time-varying demand and renewable energy uncertainty using rao-3 algorithm. *IEEE Access* **2021**, *9*, 23264–23283. [CrossRef]
47. Temperature & Solar Exposure Data for 2018. Available online: http://www.bom.gov.au/climate/data/index.shtml (accessed on 9 October 2021).
48. Solar Home Electricity Data. Available online: https://www.ausgrid.com.au/Industry/Innovation-and-research/Data-to-share (accessed on 9 October 2021).
49. Qiu, J.; Zhao, J.; Wang, D.; Dong, Z.Y. Decomposition-based approach to risk-averse transmission expansion planning considering wind power integration. *IET Gener. Transm. Distrib.* **2017**, *11*, 3458–3466. [CrossRef]